Comparison of numerical and experimental strains distributions in composite panel for aerospace applications

Waldemar Mucha*, Waclaw Kuś*, Júlio C. Viana† and João Pedro Nunes†

* Department of Computational Mechanics and Engineering
Silesian University of Technology
Gliwice, Poland
e-mail: waldemar.mucha@polsl.pl; waclaw.kus@polsl.pl

† Department of Polymer Engineering, IPC - Institute for polymers and composites
University of Minho
Guimarães, Portugal
e-mail: jcv@dep.uminho.pt; jpn@dep.uminho.pt

Key words: aerostructures, lightweight structures, strain measurement, finite element method, operational load monitoring, artificial intelligence

Abstract: *In structural applications of aerospace industry, weight efficiency, understood as minimal weight and maximal stiffness, is of great importance. This criterion can be achieved by composite lightweight structures. Typical structures for aforementioned applications are sandwich panels (e.g., with honeycomb core) and stiffened panels (e.g., with blade ribs, T-bar ribs, or hat ribs). In this paper, a hat-stiffened panel, made of carbon/epoxy woven composite, is considered. Results of experiments, consisting of loading the panel and measuring exciting forces and strains (using strain gages), are presented. The results are compared to strains distribution obtained from finite element model of the panel.*

1 INTRODUCTION

Composite lightweight structures are popularly used for aerospace applications (aircraft skin, wings etc.). They are characterized by very good weight efficiency, which means low weight and high stiffness. Typical aerostructures are sandwich panels (e.g. with honeycomb core) and stiffened panels (e.g. with blade ribs, T-bar ribs, or hat ribs) [1–5].

In aerospace applications, such structures are often monitored in real-time in order to detect potential changes to material or geometric properties which could mean potential damage (Structural Health Monitoring) [6–8], or in order to estimate the remaining in-service life of the structures (Operational Loads Monitoring) [9–12]. The monitoring is often performed by means of embedded or surface mounted strain sensors (e.g., intrinsic optical fibers or strain gages) [13, 14].

In the following paper, a hat-stiffened panel, of geometry presented in Fig. 1, is considered. Dimensions of the panel are 597 x 204 x 29 mm. The material of the panel is a 10-layer laminate – woven carbon fiber / epoxy composite. Mechanical properties of a single layer, of thickness 230 μm, are presented in Table 1.

https://doi.org/10.4995/YIC2021.2021.12572

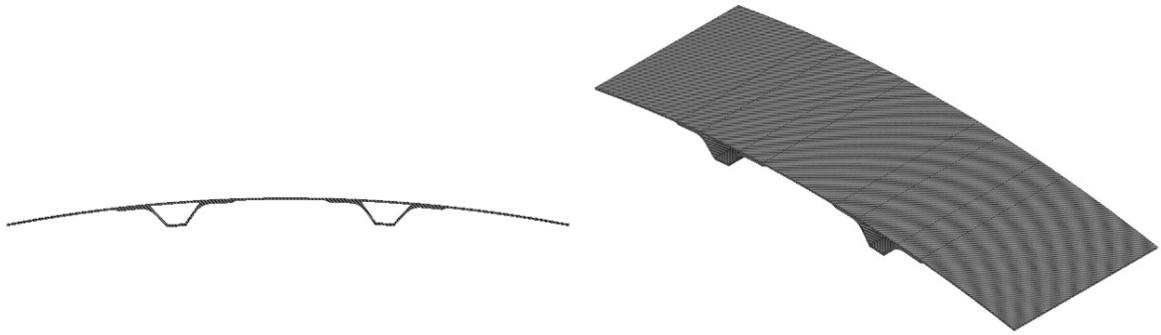

a) b)

Figure 1: Geometry of the hat-stiffened panel: a) front view, b) isometric view (597 x 204 x 29 mm).

Table 1: Mechanical properties of a single layer

Young Module	**[GPa]**	**Shear Module**	**[GPa]**	**Poisson's ratio**	**[]**
E1	64.70	G12	4.00	ν12	0.04
E2	64.70	G23	2.66	ν23	0.34
E3	7.17	G13	2.66	ν13	0.34

The geometry of the panel can be divided into the main curved part and the two ribs (Fig. 2). Each part contains 10 layers of carbon woven, therefore the panel is 2.3 mm thick (except the common part that is 4.6 mm thick). In the main part, layers 1, 3, 5, 6, 8, 10 have the carbon fibers of the woven parallel to the external edges of the panel, and layers 2, 4, 7, 9 rotated by the angle of 45°. In the ribs, all ten layers of the woven are of the same orientation – parallel to the external edges of the panel.

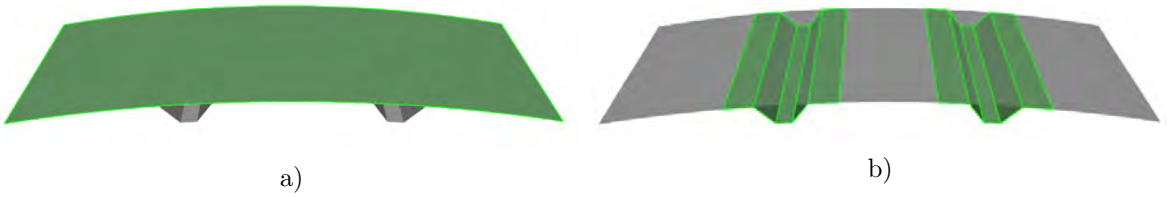

a) b)

Figure 2: Geometric regions of layer groups: a) main curved part, b) ribs.

In Section 2, the finite element model of the panel is presented, as well as results of numerical simulations for example load cases. Section 3 describes the experimental results of loading the panel and strain measurements. Strain distributions in numerical simulations and experiments are compared. Conclusions and idea of cyber-physical system for real-time monitoring of aerostructures using artificial intelligence techniques is presented in Section 4.

2 FINITE ELEMENT MODEL AND NUMERICAL RESULTS

The boundary conditions of the numerical model and characteristic points are presented in Fig. 3. On edge A displacements along axes X and Y were fixed. On edge B displacements along axis Y were fixed. Force is applied to two alternative points – F1 and F2. Displacements along axis Z are fixed in the point where load is applied. Six sensors (strain gages) are mounted at points S1-S6, to measure strains in longitudinal directions.

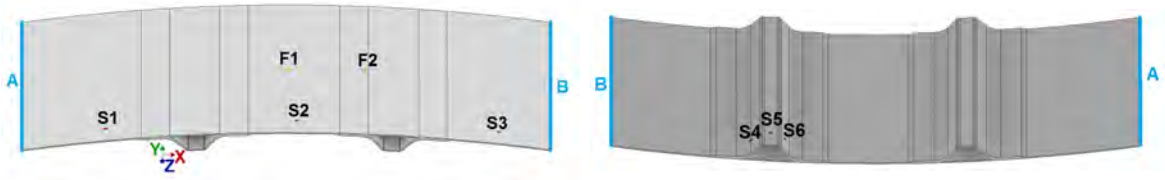

a) b)

Figure 3: Boudary conditions, strain sensors positions and load points: a) view from top, b) view from bottom.

Surface finite element model was created using ANSYS Workbench software, with ACP module. The model has got 18757 finite elements (of quadratic order) and 56584 nodes. The mesh is presented in Fig. 4. In points where loads are applied and strain sensors are mounted, the mesh is refined.

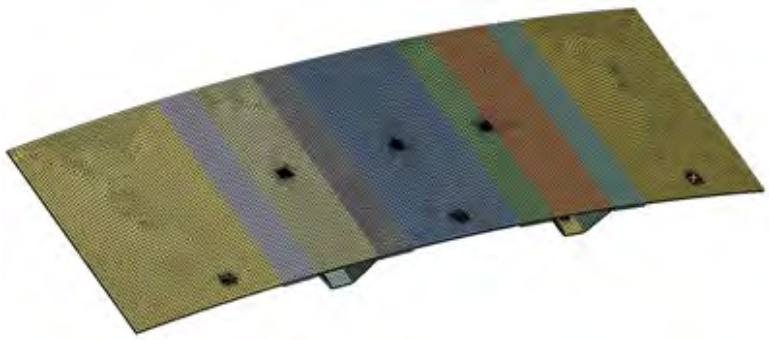

Figure 4: Finite element model.

Force of value 20 N was applied to points F1 and F2, sequentially. Displacements and strains distributions are presented in Fig. 5 and 6 for both load cases, respectively.

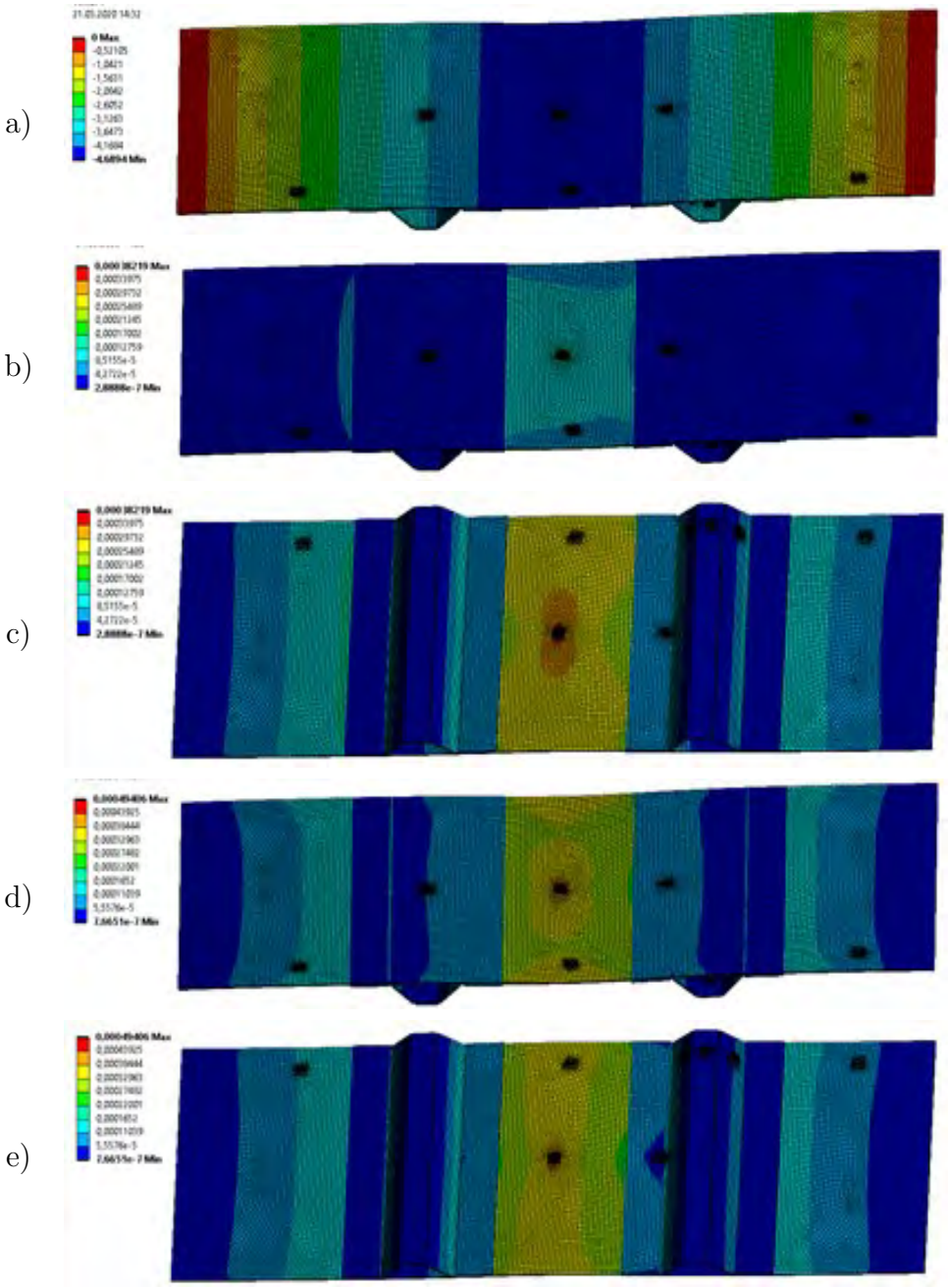

Figure 5: Results of finite element simulation, force applied at point F1 (central midpoint of the curved panel): a) vertical deformation [mm], b) maximum principal strain (top view), c) maximum principal strain (bottom view), d) von Mises equivalent strain (top view), e) von Mises equivalent strain (bottom view)

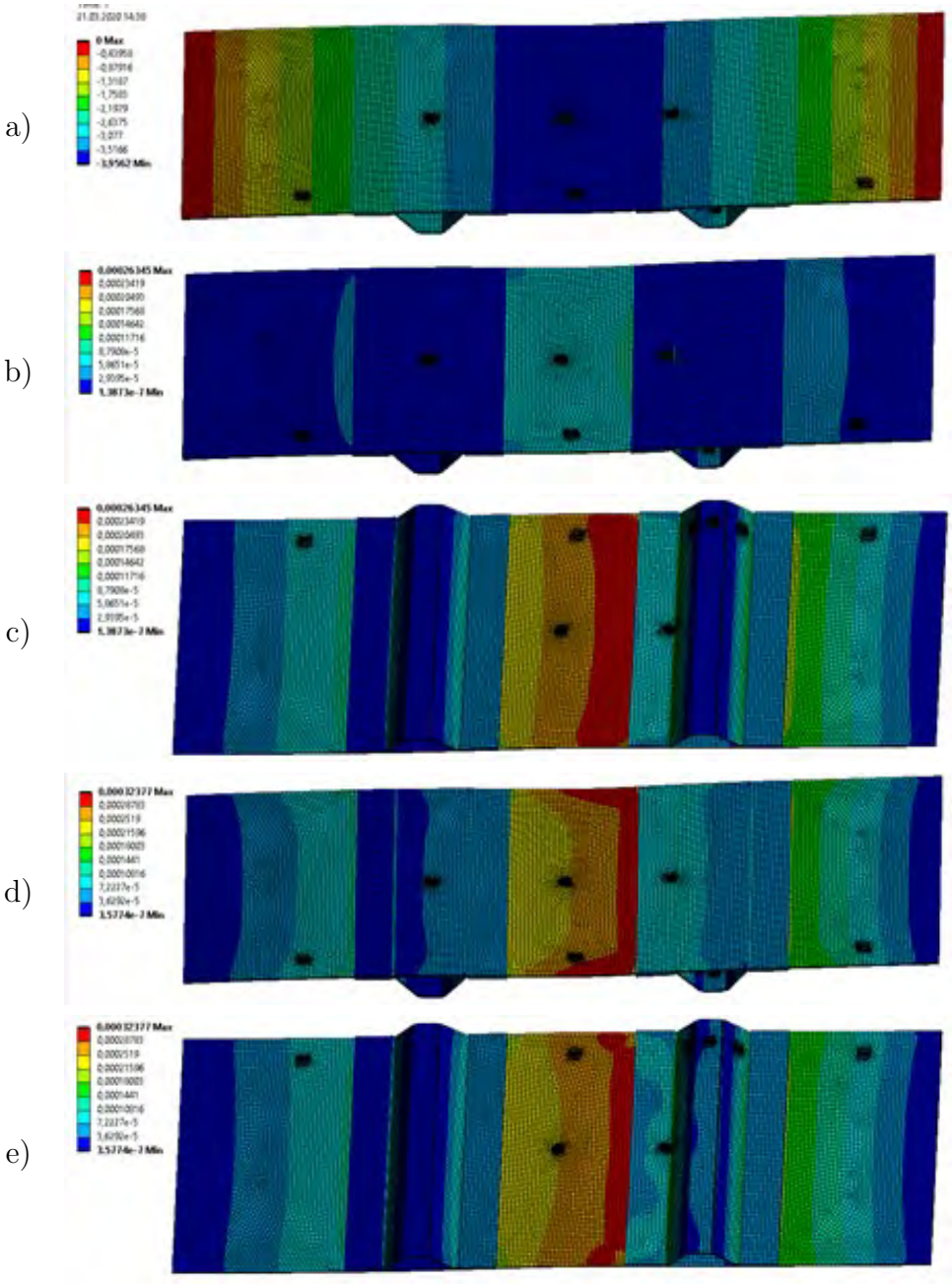

Figure 6: Results of finite element simulation, force applied at point F2 (near of the rib flap): a) vertical deformation [mm], b) maximum principal strain (top view), c) maximum principal strain (bottom view), d) von Mises equivalent strain (top view), e) von Mises equivalent strain (bottom view).

3 EXPERIMENTAL RESULTS

Experimental measurements of strains distributions were performed using a universal testing machine MTS Insight 10 with 500 N load cell and data acquisition system Hottinger Baldwin Messtechnik (HBM) MGCplus. Six strain gages and analog output of the applied load from the testing machine were connected to the acquisition system. Force was applied at points F1 and F2 in the range 0-20 N, with velocity of 0.5 mm/min. Photograph of the test stand during experiment is presented in Fig. 7.

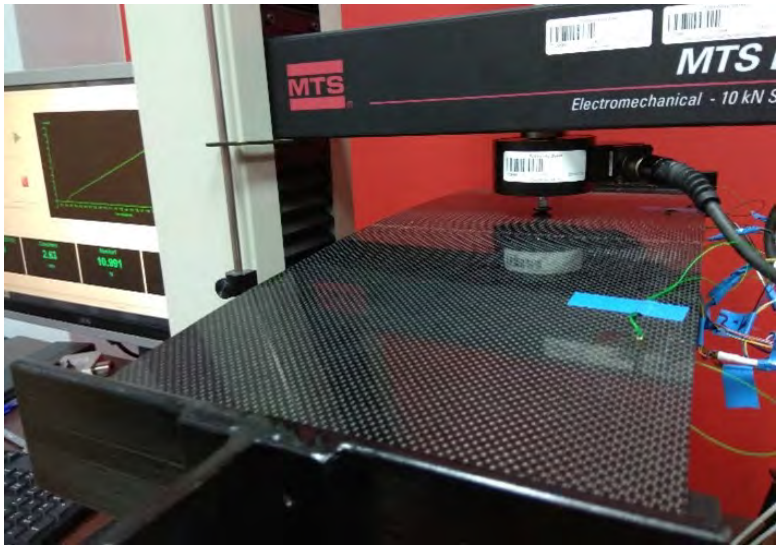

Figure 7: Photograph of experimental testing.

Strain values obtained from sensors S1-S6 during the experiments (for both load cases) were compared to numerical values. In the finite element model, the actives areas of the strain gages were modelled as separated surfaces, where average strains in local coordinate systems were computed. Comparison of the numerical and experimental data is visualized on force-strain plots, in Fig. 8. Table 2 summarizes the mean-square-errors between numerically computed and experimentally measured strains, for all strain sensors, for both load cases.

Table 2: Mean square error between numerical analysis and experimental data $[\mu m^2/m^2]$.

	S1	**S2**	**S3**	**S4**	**S5**	**S6**
F1	6.45	13.62	2.40	4.08	0.60	1.44
F2	12.18	48.30	5.95	1.56	1.99	12.60

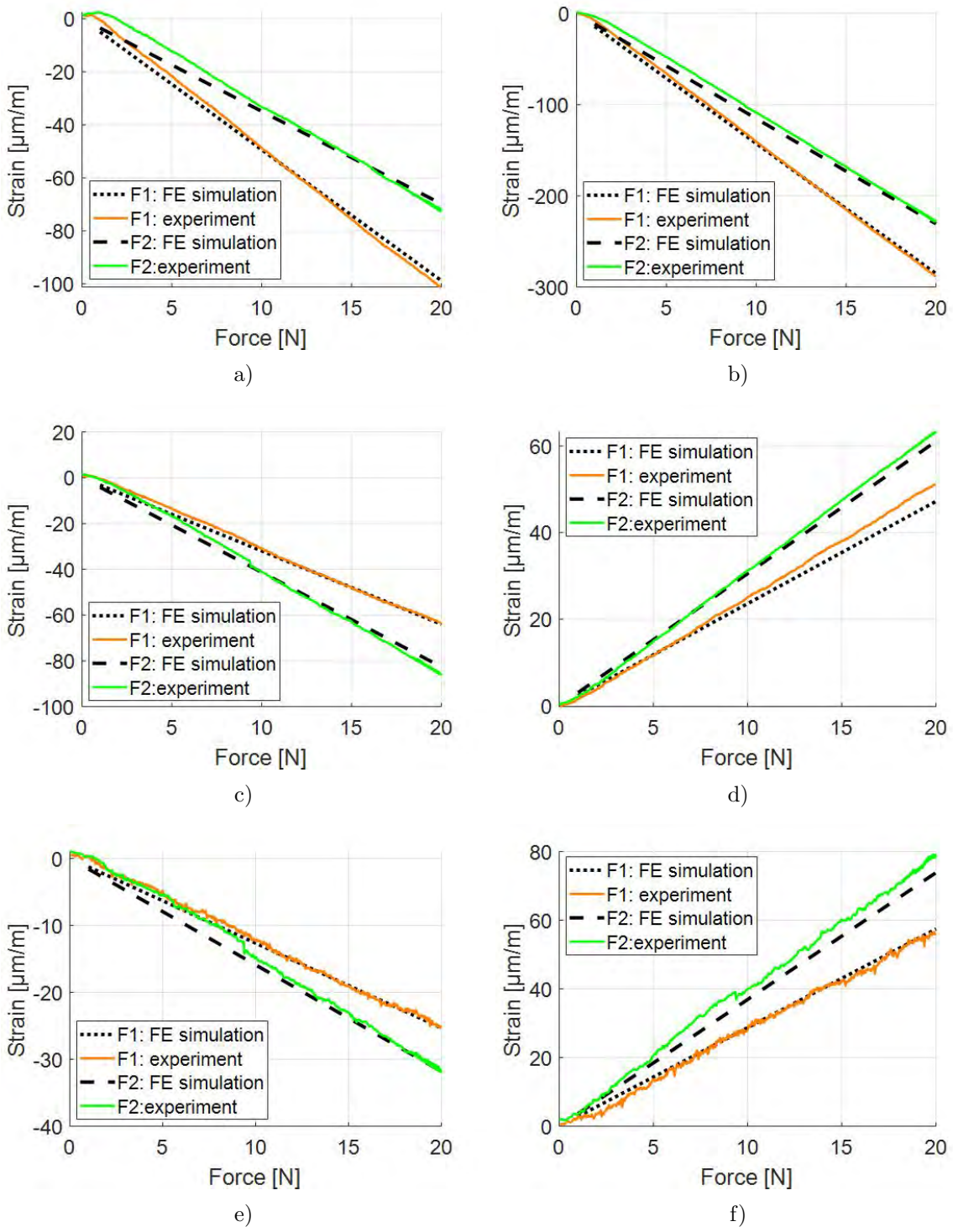

Figure 8: Comparison of strains obtained from experiments and numerical simulations: a) S1, b) S2, c) S3, d) S4, e) S5, f) S6

4 CONCLUSIONS

As one can see in Figures 8 and 9 and in Table 2, quite good agreements between numerical and experimental results were obtained. The finite element model is of satisfying accuracy. Minor differences between computed and measured strains can result from measurement accuracy of strain gages, material imperfections of the prototype panel (related to manufacturing process), minor geometrical differences between model and prototype.

The obtained results are for the authors a starting point for future research on real-time monitoring system. The idea is a cyber-physical system (CPS, system where computing unit controls physical components) [15], whose goal is real-time monitoring of aerostructures in order to predict possible damage, current loading state, or life span of the structure, based on strain measurements in selected areas. The number of critical points, where measurements should be taken, may be sometimes very high. In order to decrease the number of sensors, artificial intelligence techniques will be introduced. Artificial neural networks (ANNs) or deep learning networks (DLNs) will be trained, based on FE model of the structure, to give information on the whole structure, based on measurement data of only few points. The necessary condition is a high fidelity numerical model, that provides very similar data as the real object, like the model presented in the paper. Real-time computations using ANNs could be even performed in the microcontroller [16] on which the CPS is built.

REFERENCES

[1] G.-H. Kim, J.-H. Choi, and J.-H. Kweon, "Manufacture and performance evaluation of the composite hat-stiffened panel," *Composite Structures*, vol. 92, no. 9, pp. 2276–2284, 2010, fifteenth International Conference on Composite Structures.

[2] Y. M. Tang, A. F. Zhou, and K. C. Hui, "Comparison of fem and bem for interactive object simulation," *Computer-Aided Design*, vol. 38, no. 8, pp. 874–886, 2006.

[3] B. Zalewski and B. Bednarcyk, "Act payload shroud structural concept analysis and optimization," National Aeronautics and Space Administration, Cleveland, Ohio, USA, Tech. Rep., 2010, nASA/TM—2010-216942.

[4] K. Pravallika and M. Yugender, "Structural evaluation of aircraft stiffened panel," *International Journal of Science and Research*, vol. 5, no. 10, pp. 753–759, 2016, paper ID: ART20162160.

[5] M. P. Arunkumar, J. Pitchaimani, K. V. Gangadharan, and M. C. Lenin Babu, "Influence of nature of core on vibro acoustic behavior of sandwich aerospace structures," *Aerospace Science and Technology*, vol. 56, pp. 155–167, 2016.

[6] E. P. Carden and P. Fanning, "Vibration based condition monitoring: A review," *Structural Health Monitoring*, vol. 3, no. 4, pp. 355–377, 2004.

[7] M. Mitra and S. Gopalakrishnan, "Guided wave based structural health monitoring: A review," *Smart Materials and Structures*, vol. 25, no. 5, p. 053001, 2016.

[8] W. Fan and P. Qiao, "Vibration-based damage identification methods: A review and comparative study," *Structural Health Monitoring*, vol. 10, no. 1, pp. 83–111, 2011.

[9] N. Aldridge, P. Foote, and I. Read, "Operational load monitoring for aircraft & maritime applications," *Strain*, vol. 36, no. 3, pp. 123–126, 2008.

[10] A. Kurnyta, W. Zielinski, P. Reymer, and M. Dziendzikowski, "Operational load monitoring system implementation for su-22um3k aging aircraft," in *Structural Health Monitoring 2017*, Stanford, California, USA, 2017.

[11] V. Giurgiutiu, "Shm of fatigue degradation and other in-service damage of aerospace composites," in *Structural Health Monitoring of Aerospace Composites*, V. Giurgiutiu, Ed. Oxford: Academic Press, 2016, ch. 10, pp. 395–434.

[12] S. Willis, "Olm: A hands-on approach," in *ICAF 2009, Bridging the Gap between Theory and Operational Practice*, M. J. Bos, Ed. Dordrecht: Springer Netherlands, 2009, pp. 1199–1214.

[13] D. C. Betz, W. J. Staszewski, G. Thursby, and B. Culshaw, "Multi-functional fibre bragg grating sensors for fatigue crack detection in metallic structures," *Proceedings of the Institution of Mechanical Engineers, Part G: Journal of Aerospace Engineering*, vol. 220, no. 5, pp. 453–461, 2006.

[14] S. Lecler and P. Meyrueis, "Intrinsic optical fiber sensor," in *Fiber Optic Sensors*, M. Yasin, S. W. Harun, and H. Arof, Eds. Rijeka: IntechOpen, 2012, ch. 3, pp. 53–76.

[15] W. Kuś and W. Mucha, "Memetic inverse problem solution in cyber-physical systems," in *Advances in Technical Diagnostics*, A. Timofiejczuk, B. E. Łazarz, F. Chaari, and R. Burdzik, Eds. Cham: Springer International Publishing, 2018, vol. 10, pp. 335–341.

[16] W. Mucha, "Real-time finite element simulations on arm microcontroller," *Journal of Applied Mathematics and Computational Mechanics*, vol. 16, no. 1, pp. 109–116, 2017.

ACKNOWLEDGEMENT

The research was partially funded from financial resources from the statutory subsidy of the Faculty of Mechanical Engineering, Silesian University of Technology, in 2021.

W.M. acknowledges the National Agency for Academic Exchange of Poland (under the Academic International Partnerships program, grant agreement PPI/APM/2018/1/00004) for supporting training in the University of Minho, which enabled execution of the study.